Enhancing the performance of radial distribution systems via optimal integration of electric vehicles

Afaf Rabie, Abdelhady Ghanem, Sahar S. Kaddah, Magdi M. El-Saadawi
Department of Electrical Engineering, Faculty of Engineering, Mansoura University, Mansoura, Egypt

Article Info

ABSTRACT

Electric vehicles (EVs) and their associated charging stations (CSs) are a promising avenue for greenhouse gas reduction and energy security. However, improper location and size of the EV charging station (CSs/EVs) negatively affect the power system. It results in some technical challenges such as increased real power-loss, decreased voltage stability and increased voltage deviation. This paper suggests optimum planning of CSs/EVs locations to conserve voltage, improve power-loss and reduce the effect of CSs/EVs in electrical distribution systems. The multi objective genetic algorithm method (MOGA) is utilized to solve the optimization problem and reduce the impact of the random location of CSs/EVs. The simulations are performed on IEEE 33-bus and IEEE 69-bus radial distribution systems (RDS). In addition, the optimal EV allocation is carried out with two fixed levels of loading from 100% to 150% of the candidate EV load. A comparison between the proposed MOGA technique and other optimization techniques is carried out. The results demonstrated the capability of the proposed technique for optimal placement of CSs/EVs in RDS. Moreover, it is providing an objective value to solve a complex multi-objective nonlinear optimization problem to reduce the total power-loss, improve the voltage profile and extend the voltage stability.

Corresponding Author:

Abdelhady Ghanem
Department Electrical Engineering, Faculty of Engineering, Mansoura University
El Gomhouria St, Dakahlia Governorate, Mansoura 35516, Egypt
Email: aghanem_m@mans.edu.eg

1. INTRODUCTION

Globally, electric vehicles are one of the best ways to reduce pollution. The economic and environmental problems of transporting fossil fuels have spurred the electrification of vehicles around the world. Moreover, many expected benefits are also increasing as technology improved [1]. The electric vehicles (EVs) market share reached 28.8% in Norway, 6.4% in the Netherlands and 1.4% in China, whereas many countries have set targets to reach 100% EV penetration in the foreseeable future [2]. By 2025, the number of global EVs is expected to surpass 40 million [3]. If this rate continues until 2050, EVs will replace 62% of fleet vehicles [4]. Researchers highlighted the significant impact of switching from conventional vehicles to EVs to reduce the transportation sector's contribution to greenhouse gases, due to the lower costs of electricity compared to fossil fuels [5]. One of the drawbacks of EVs is their limited driving range. The EV batteries state of charge (SOC) reduces while EVs are moving, and hence need to be linked to the grid for recharging [6]. Therefore, there is a great emphasis on the establishment of large-scale EV charging stations [7]. It is worth noting that the appropriate location of EV charging stations is critical to preventing detrimental impacts on power quality [8]. EVs are mostly related to the distribution voltage level. With high EV penetration, the load flow of energy changed not only in the distribution system, but also in the transmission subsystem [9].

Deployment of charging station (CS) infrastructure is the most important for EV technology, and location of the CSs will bring new challenges to power supply systems if technical specification is not considered during the planning process. Academia and industry are moving towards proper CSs planning in electrical systems [10]. Generally, many optimization algorithms are used to solve the problem of locating the electric vehicles' charging stations (CSs/EVs). It usually focuses on maximizing customer needs or reducing travel costs [4]. In addition, many public transportation vehicles depend on renewable energy sources, so in some areas the photovoltaic system is set up to efficiently charge interchangeable battery systems [11].

A review on determining the optimal location of EV charging station infrastructure and its model classification based on transmission and distribution systems is presented in [12]. The work in [13] explain an optimal place of the electric vehicle charging station in a transmission network is determined considering the EV Leadership range, which sub-edited the problem of the road node covering (RNC). Furthermore, results show that the selection of an intelligent path, flexibility and efficiency of the design can select optimal locations for CSs from different potential locations without difficulties. According to [14], the CS/EV site in Sweden is planned to use geographical information system (GIS) depending on traffic flux average and earth sorting data. The problem of optimization is dealt with combined linear and integer programming to maximize revenues using the new CS/EV. The charging station infrastructure and its location are defined for the transportation network in Italy considering features of the highway and driving behavior in [15]. Moreover, depending on service venture and risk, the sites and sizes of CSs are specified utilizing whale optimization algorithm (WOA) [16]. The optimal locations of CS/EVs are determined in [2] based on the particle swarm optimization (PSO) algorithm. The objective function is solved considering planning time, the overall cost of the CSs (i.e., development, operation, and repairing) as well as voltages and current limitations. Depending on the EVs transportation cost and the performance of the system, the optimal assignment of the EV charging problem is elaborated in [17]. The location problem of fast charging stations is settled in [18]. The presented work uses the candidate places with investment operation in the supreme network considering the effect of EV stations on motorists, traffic status, losses power of EVs and operation in the low voltage network. The locations of fast charging stations are suggested for a 123-bus distribution network in [19] using multi-objective grey wolf optimizer (MOGWO) algorithm considering transport system limits. In addition, an optimal site of charging stations in presents of capacitors is proposed in view of power loss and voltage profile improvement in electric distribution networks [20]. Moreover, other algorithms have studied the optimal position of CSs/EVs in radiation distributed systems. The result in [21], depending on transformer ratings and the determination of available EV numbers, the 107-bus residential low-voltage distribution system is analyzed in real time to locate CSs/EVs optimally. The cost of charging is reduced by the algorithm of salp swarm (SSA), considering the technical constraints of the network under classical and smart modes of charging. The results demonstrated that the voltage deviation due to increasing EV loads in secondary feeders is higher than the primary feeder deviation. The effect of EV charging on the distribution network is reduced by designing policies for EV charging with the objective function of reducing the cost of operation, EV penetration and overall losses. The cost function is defined with two components. The first is specified as the aging of the transformer and the second component coincided with distribution system losses [22]. In addition, depending on actual data, a financial cost of charging batteries has been added to the cost index as a third component which regards the EV itself [23]. While the simulation proved that the proposed policy for EV charging worked quite likewise the current charging policies. However, it discovered more origins of the profiles in the existence of predictive errors. Moreover, the study in [24], identified the optimal location of a number of fast charging stations in the American network to serve 10% of EV load penetration without exceeding network operational constraints like voltage levels and harmonic distortions. The analysis includes the geographical, social, and technical sides of defining the infrastructure needed to model a fast EV charging station of a 50 kW with a DC/DC and AC/DC power converter. On the other hand, the CS demand for spread EVs was estimated in [25] depending on a probabilistic model or by an approximate model for improving reliability in the system. In [25], the required power for CSs/EVs are determined according to the EVs' demand power that mainly depends on the number and types of charging ports. Hence, according to various charging schemes, the smart charging method is suggested to reduce the cost of operation at the peak require while maintaining reliability and network security agents [26]. From this, it was necessary to plan the increasing EVs penetration on the distribution networks appropriately to upgrade the economic and technical benefits and raise EV penetration rate as presented in [27]. Due to EV power change depending on its type, multiple charging ports (CPs) are established for several types of EVs achieving economic targets and raising penetration level of EVs [28]. Furthermore, various types of AC and DC models and power demand characteristics are reviewed in [29]. In view of the above works, MOGA and voltage stability index (VSI) are utilized to customize CS/EV in a distribution system considering system improvements. VSI is utilized to reduce active power losses by identifying candidate buses. While GA produces a new generation of chromosomes and calculates fitness values of improving the voltage profile and voltage stability enhancing. The algorithm has been tested on 33-bus and 69-bus systems with CS/EV load.

The efficiency of the proposed algorithm is simulated with different scenarios. The rest of this paper is arranged as follows. In section 2, the mathematical model of the problem is presented. The objective function as well as its constraints are discussed in section 3. In section 4, details of the proposed optimization method using MOGA are illustrated. Simulation results and analysis of different operating scenarios are presented in section 5. Finally, some conclusion remarks are provided in section 6.

2. PROBLEM FORMULATION

In order to reduce the effect of EV load on the performance of the radial distribution system, the CSs/EVs are located optimally using MOGA. The load flow analysis of RDS is performed using the back-and-forward sweep [30]. The elements of the multi objective function (MOF) that include the reduction of real power loss, enhancing voltage stability and optimizing voltage profile are debated as follows:

2.1. Minimizing real power loss

The first component of the objective function is minimizing actual power loss (PL), F_1 which is determined in (1).

$$F_1 = \text{reducing} (P_{Loss})$$ (1)

The active power losses are defined by summing up all losses in the branches as given in (2).

$$P_{Loss} = \sum_{i=1}^{Nbs} \left(\frac{(P_i^2 + Q_i^2)}{|v_i|^2} \right) * r_{ij}$$ (2)

For i is the sending end node and j is the receiving end node.

2.2. Minimizing voltage deviation index

The second component F_2 of the objective function is minimizing the voltage deviation index. The voltage deviation index (VDI) is introduced to evaluate the improvement that occurs in the voltage profile, which can be determined as the disparity between the nominal voltage and the actual voltage. The VDI can be evaluated using the following expression [30], [31].

$$VDI = \frac{1}{Nbs} \sum_{i=1}^{Nbs} \left| \frac{V_{ni} - V_i}{V_n} \right|$$ (3)

Where V_{ni} is nominal voltage of the ith bus. Usually, it is taken as V_n= 1.0 p.u. and the ith bus voltage magnitude is V_i.

2.3. Voltage stability index

The third component F_3 of the objective function is the voltage stability index (VSI) which used as an indicator of system stability and load ability. As indicated in [32], the voltage stability index (VSI) of a branch can be defined depending on the magnitude of voltage of the sending bus, active and reactive power for loads at the receiving bus and the resistance of lines and reactance. VSI can be estimated as given in (4).

$$VSI_i = \left[|V_j|^4 - 4(P_i x_{ij} - Q_i r_{ij})^2 - 4(P_i r_{ij} - Q_i x_{ij}) |V_j|^2 \right]$$ (4)

When VSI for all the buses are more than zero, the system stability is achieved. VSI of minimum value is addressed as the overall stable condition of the system [9]. Improved VSI (F_3) can be realized as shown in (5).

$$F_3 = Maximize(VSI) = Minimize \left(\frac{1}{(VSI)} \right)$$ (5)

3. OBJECTIVE FUNCTION FORMULATION

An optimization problem involving more than one objective is called a multi-objective optimization problem [30]. All measured objective functions are integrated to form a multi-objective function (MOF) as presented in (6) in order to minimize the losses, improve the voltage stability index and reduce the voltage deviation.

$$MOFi = \min (w_1 F_1 + w_2 F_2 + w_3 f F_3)$$ (6)

Where w_1 to w_3 are weighting constants appropriated to each objective and their summation must equal unity [33]. The constraints that achieve optimization of the multiple goals are mentioned in the next section [31].

The multi-objective function presented in (6) can be achieved along with inequality and equality constraints. The operational bus-voltage boundaries V_i and power flow S_i and the charging station (CSs/EV) design constrains such as the number of charging ports and (CSs/EV) number are considered as (7).

$$NCP_{min} \leq NCP \leq NCP_{max}$$

$$NCS_{min} \leq NCS \leq NCS_{max} \tag{7}$$

Where (NCP) and (NCS) are the number of EV charging ports and number of EV charging stations respectively. NPC and NCP boundaries should be between the minimum and maximum permissible limits. The algorithm of load flow is provided to set the values of the optimization function defined in the MOF while the MOGA algorithm considers the constraints while realizing the MOF.

4. PROPOSED ALGORITHM

In this paper, it is proposed to utilize an improved genetic algorithm (GA) in order to customize CS/EV in a distribution system considering system improvements. The objective function is defined as a multi-term objective function as formulated in section 2. Generally, GA is a generalized optimization technique based on the theory of biological growth and natural genetics. Unlike conventional methods that involve iterative changes to a single solution, GA works with a set of solutions and the candidate solutions to the problem are preserved by a set of individuals represented by GA [34]. In the following subsections, details of multiple objective genetic algorithm (MOGA) based optimal utilization of CS/EV in a distribution system is presented.

4.1. Multiple objective genetic algorithm (MOGA)

MOGA is an extension of the basic GA algorithm in order to solve multi-object optimization problems in various fields [35]. It uses different specified random weights of multiple objective functions which can be combined into a scalar fitness function. Once the determination of the fitness is obtained, selection can be done and utilization of conventional GA can be followed. For the solution S_i of a multi-object problem, a rank amount to one is assigned and added to the number of solutions n_{S_i} which dominates solution S_i. Each rank-solution is considered simultaneously, and their initial fit is averaged. This average fit is now called the custom fit for each mattress solution in (8).

$$F_i = N - \sum_{r_{Si}=1}^{r_{Si}-1} \mu(r_{Si}) - 0.5(\mu(r_{Si}) - 1) \tag{8}$$

Where $\mu(r_{Si})$ is the number of solutions in a rank r_{Si} and Si =1, 2, …, N.

This confirms the non-dominant solutions in the population. To keep diversity among the non-dominant solutions, appropriate solutions are given for each rank by calculating the niche count by collecting the values of sharing function as shown in (9).

$$nc_{Si} = \sum_{Sj=1}^{\mu(r_{Si})} sh\left(d_{SiSj}\right) \tag{9}$$

Where, $sh\left(d_{SiSj}\right)$ is the sharing function value of two solution S_i and S_j. The sharing function is set based on the objective function as a measure of distance as (10).

$$sh\left(d_{SiSj}\right) = \begin{cases} 1 - \left(\frac{d_{SiSj}}{\sigma_{share}}\right)^\alpha & d_{SiSj} \leq \sigma_{share} \\ 0 \; otherwise \end{cases} \tag{10}$$

The σ_{share} is the exchange element which indicates the extreme dimension between any pair solutions before they meet at the similar niche. α is a scaling agent less than or equal to one, and d_{SiSj} is the settled distance between pair of solution S_i and S_j. Hence, the membership function for undefined solutions is evaluated as (11),

$$\mu^k = \frac{\sum_{i=1}^{N_{obj}} \mu_i^k}{\sum_{k=1}^{M} \sum_{i=1}^{N_{obj}} \mu_i^k} \tag{11}$$

Where M is the number of undefined solutions and N_{obj} is the number of targets. Finally, the finest compromise is the one that increases the functionality of the membership.

4.2. Applying MOGA to solve optimization problems in RDS with CSS/EVS

In this part, CSs/EVs sites are identified to reduce system losses and improve VSI using MOGA. MOGA proceeds in several directed steps as shown in Figure 1 that describes the flow chart of the proposed algorithm.

i) Step 1: Firstly, the multi-objective function that is subject to all constraints of the system variables is identified.

ii) Step 2: Initialize the chromosome population size that equals to the number of individuals and layout variables including the number of CS/EV, sizes in kW, and the first position in the network for each CS/EV.

iii) Step 3: Assess fitness by running load flow, performing an initial evaluation of individuals/the population, and determining the multi objective function values (MOF) in (6).

iv) Step 4: Define iteration g=1 and select the better population/individual that provided the best MOF and handle these individuals as decent. Also, identify the average of the entire population for ranking, and sharing.

v) Step 5: Update existing solutions by substituting the mutation with one or some specific coordinates. And if the solutions lead to acceptable results than the existing ones, proceed with all confirmed solutions.

vi) Step 6: Modify the acquired solutions from the previous step, check the fit, and select the confirmed solutions after crossover if they lead to acceptable solutions than the existing ones.

vii) Step 7: Keep the best present individuals and repeat the steps (4) through (6) until the maximum number of iterations is reached and the convergence point is attained.

viii) Step 8: Finally, print the best solution/MOF as a perfect result, plot the preserved parameters that were recorded for all iterations as affinity properties then stop. Figure 1 shows a flow chart of the proposed algorithm.
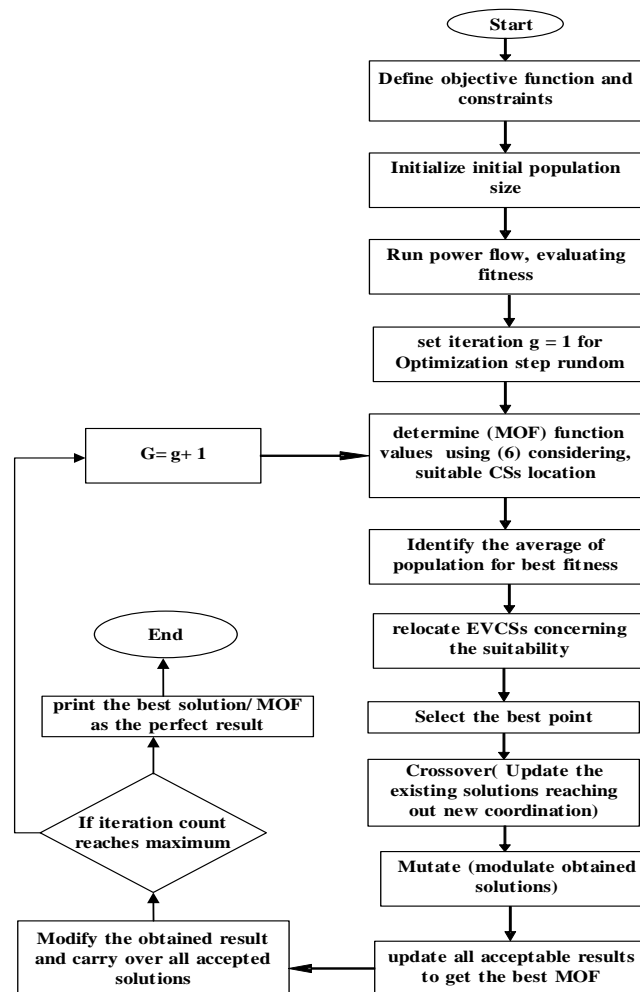

Figure 1. Flow chart of the proposed algorithm

5.   SIMULATION RESULTS

Depending on the methodology proposed, the algorithm software tool was built in the MATLAB environment to run the load flow and identify the best location of CSs/EVs that reduces the active power loss and improves the stability. The simulation results are described as an algorithm analysis of the technical benefits of the IEEE 33-bus system and the tested RDS 69-bus systems, and the system's data are taken from ref [36], [37]. The MOGA parameters contain three unknown variants number in the space of search (for 3 locations of CS/EV), maximum number of iterations is 100, and the population number is 30. Initial crossover and mutation are 0.95, and 0.01 respectively.

To demonstrate the effectiveness of the proposed algorithm different models of EV have been added in the CS design considering the charging ports (CPs) for AC/DC type 2 of charging as shown in Table 1 (Chevrolet VOLT, BMW I3, Tesla Model X, Chang an Yidong). The intended CP type is suitable for both hybrid electric vehicles (PHEVs) and battery electric vehicles (BEVs) under SAE J1772 standard, with a maximum rated power of 7 kW [38]. Table 1 details CPs features such as the EVs types and the rated power for each type that can be charged simultaneously in a specific CS, as well as the maximum and minimum number of CPs for the various EVs types and the appropriate maximum and minimum rated power for the CS [1], [29], [39].

Table 1. Features of simulator charging stations of electric vehicles (CSs/EVs)

Category of EV	Rated power of EV (kW)	EV number		CS/EV rating power (kW)	
		Min	Max	Min	Max
Chevrolet Volt	2.20	25	35	55.0	77.0
BMW i3	44.0	10	20	440.0	880.0
Tesla model X	13.0	15	25	195.0	325.0
Saej1772 standard	7.0	30	40	210.0	280.0
Chang an Yidong	3.80	20	30	75.0	112.50
Total power rating of CSs/EVs (kW)		100 EV	150 EV	975 kW	1674.50 kW

For the designed CSs the minimum power rating of one CS is 975 KW as shown in Table 1. Comparably the demand power rating increased to 1675.5 KW for the maximum power of the CS. The following scenarios are approaches to address the results and show the effectiveness and quality of the MOGA algorithm.
i)   Scenario 1: Base case without CS/EV
ii)   Scenario 2: Adding three minimum CS/EV (300EV) without optimal location
iii)   Scenario 3: Adding three minimum CS/EV (300EV) with optimal location
iv)   Scenario 4: Adding two min CSs and one max CS (350EV) without optimal location
v)   Scenario 5: Adding two min CSs and one max CS (350EV) with optimal location
vi)   Scenario 6: Adding one min CSs and two max CS (400 EV) without optimal location
vii)   Scenario 7: Adding one min CSs and two max CS (400 EV) with optimal location
viii)   Scenario 8: Adding three maximum CS (450 EV) without optimal location
ix)   Scenario 9: Adding three maximum CS (450 EV) with optimal location
The above scenarios are applied to two different systems namely, IEEE 33-Bus System and IEEE 69-Bus system.

5.1.   Simulation results for IEEE 33-bus system

The 33-bus system [36] is presented in Figure 2 containing a primary feeder (slack bus), three laterals and 32 branches that have 3715 kW real power and reactive power loads equal to 2300 kV with 12.66 kV as operating voltage. The conventional power flow studies are not suitable for determining line flow and bus voltage in RDS. The back/forward sweep (BFS) algorithm is one of the effective methods for RDS for energy flow studies. By applying the previous scenarios on this system, the results are listed in the following subsection.

5.1.1. Scenario 1: Base case without CS/EV

When carrying out the load flow for the base case, the real power loss is 210.99 kW (5.675% of the system's active power) while the reactive loss is 143.03 kVAR. The minimum voltage is observed at bus 18 (0.9042 pu) with a minimum voltage stability index (VSI) of 0.67036 p.u. Moreover, in this simulation, the average (AVDI) voltage deflection index is 0.00393 p.u and the system voltage deviation is 9.621%.

5.1.2. Scenario 2: Adding three minimum CS/EV (300 EV) without optimal location

In this scenario, three CSs are connected as concentrated load in a sub-feeder randomly to the system. The estimated load demand is increased by 2925 kW, as given in Table 1, increasing the active load to 1.78731 times the original condition. The losses were increased from 210.99 kW to 570.1210 kW raising

the original load flow in the first scenario to 63.379%). The minimum voltage still occurs at bus 18 has been reduced from 0.9042 p.u to 0.8950 p.u. Therefore, the average (AVDI) voltage deflection index is raised to 0.00962 from 0.00393, also the decreasing of stability index (VSI) was observed from 0.67036 to 0.6333.
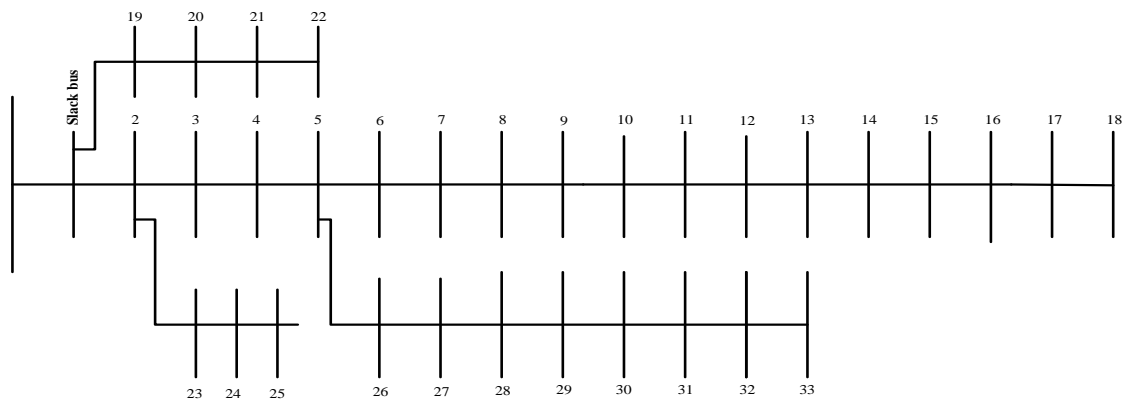

Figure 2. 33-Bus test distribution system

5.1.3. Scenario 3: Adding three minimum CS/EV (300 EV) with optimal location

By applying the optimization algorithm, the CSs/EVs best locations are at buses (2, 19 and 25). The real power losses have been reduced from 570.1210 kW to 295.0750 kW, there is a clear increase in voltage at bus 18 from 0.8950 p.u to 0.9019 p.u as shown in Figure 3, the voltage stability index is upgraded from 0.6333 to 0.654631 as shown in Figure 4. By monitoring the results, the average voltage deviation index is decreased to 0.003064 from 0.00962 and the losses have been reduced by 48.24% when compared to the losses in scenario 2. Comparing the results for scenarios 1, 2 and 3 is illustrated in Table 2.
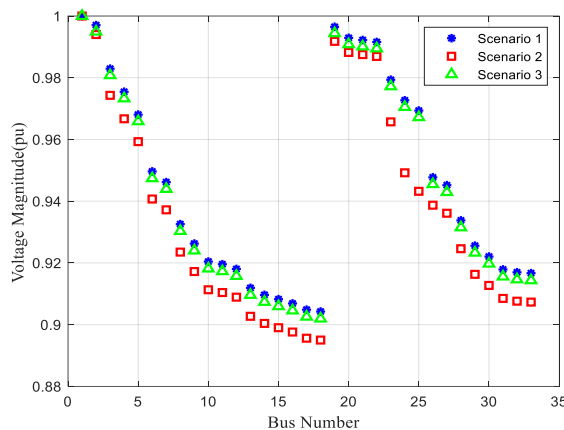
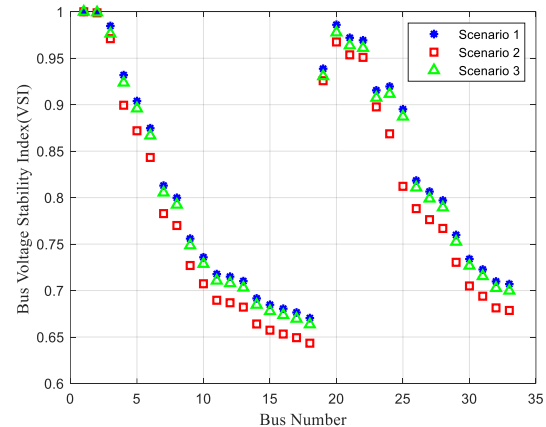Figure 3. Per unit voltage of 33-bus system with scenarios 1, 2 and 3

Figure 4. Voltage stability index of 33-bus system with scenarios 1, 2 and 3

Table 2. Performance indices comparison for 33- bus system (scenarios 1, 2 and 3)

System	Scenario	P-loss (kW)	VSImin (P.U)	Vmin (P.U)	AVDI (P.U)
33 buses	Scenario 1	211	0.67036	0.9042	0.00393
	Scenario 2	570.1210	0.6333	0.8950	0.00962
	Scenario 3	295.0750	0.654631	0.9019	0.003064

5.1.4. Scenario 4: Adding two min CSS and one max CS (350 EV) without optimal location

For a total EV load of a three CS/EV consisting of two min and one max number of CPs/CS (about 350 EV). By estimating the total power demand of EV from Table 1 which equal to 3624.5 kW integrated to the system without optimization. Thus, total load in the system is increased to 7339.5 kW from 3715 kW

(which was 1.97564 times the original load). Since the EV load is integrated randomly without optimal site planning, losses were increased from 210.99 kW to 570.526 kW raising the original load flow in the first scenario to 63.192%). As shown in Figure 5, the voltage on bus 18 has been reduced from 0.9042 p.u to 0.8917 p.u. Therefore, the AVDI is raised to 0.00983 from 0.00393, also VSI is decreased from 0.67036 to 0.6258 as shown in Figure 6.

5.1.5. Scenario 5: Adding two min css and one max CS (350 EV) with optimal location

In this case, the CSs/EV best locations are at buses (2,19 and 25) by applying the optimization algorithm for the same load of scenario 4. The real power losses have been reduced from 570.526 kW to 302.09 kW, there is a clear increase in voltage at bus 18 from 0.8917 p.u to 0.9015 p.u, the VSI is upgraded from 0.6258 to 0.6533, and AVDI is decreased to 0.00384 from 0.00983. By monitoring the results as illustrated in Table 3, the losses have been reduced by 47.051% when compared to the losses in scenario 4. Figures 5, and 6 indicate the bus voltage profile and the stability index in the case of connecting 350 EVs to the 33-bus system.
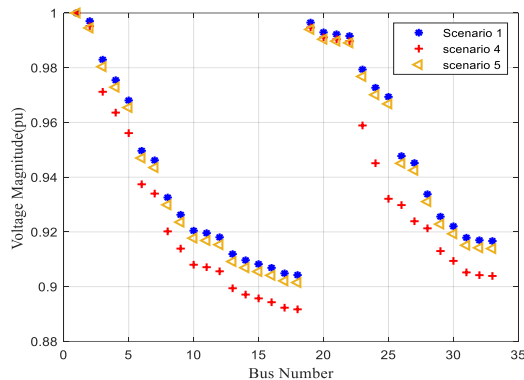

Figure 5. Per unit voltage of 33-bus system with scenarios 1, 4 and 5
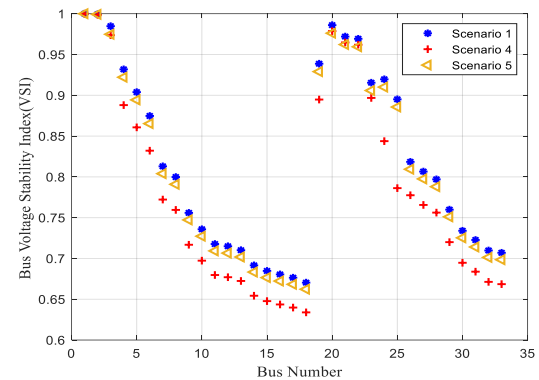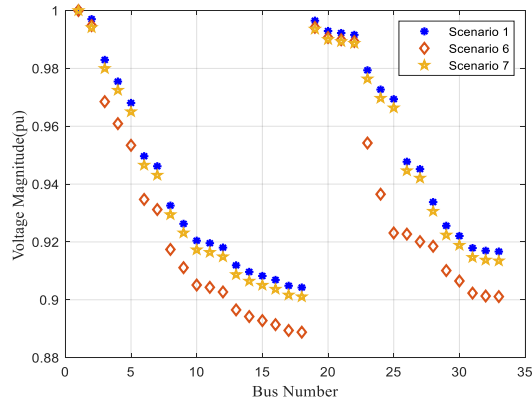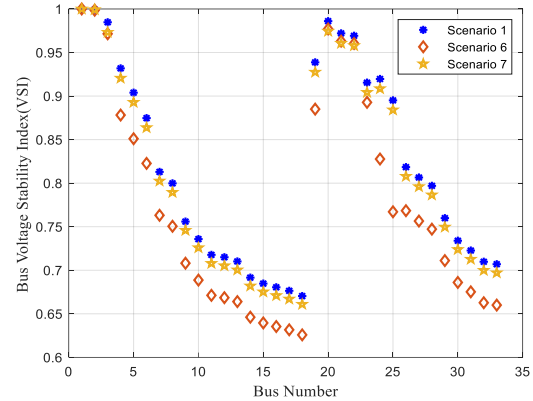
Figure 6. Voltage stability index of 33-bus system with scenarios 1, 4 and 5

Table 3. 33 Performance indices comparison for 33- bus system (scenarios 1, 4 and 5)

System	Scenario	P-loss (kW)	VSI*min* (P.U)	V*min* (P.U)	AVDI (P.U)
33 buses	Scenario 1	210.99	0.67036	0.9042	0.00393
	Scenario 4	570.526	0.6258	0.8917	0.00983
	Scenario 5	302.09	0.6533	0.9015	0.00384

5.1.6. Scenario 6: Adding one min CSS and two max CS (400 EV) without optimal location

By adding 400 EVs with a load demand of 4324 kW to the 33-bus system. Thus, the total load in the system is increased to 8039 kW from 3715 kW (which is 3.16393 times the original load). Since the EV load is integrated randomly, losses are increased from 210.99 kW in the base case to 690.66 kW raising the original load flow in the first scenario to 69.451%) as listed in Table 4. The voltage on bus 18 has been reduced from 0.9042 p.u to 0.8886 p.u. Therefore, the average (AVDI) is raised to 0.0103 from 0.00393, and a decrease from 0.67036 to 0.6172 in the stability index (VSI) is observed.

5.1.7. Scenario 7: Adding one min CSS and two max CS (400 EV) with optimal location

Hence, the goal of optimizing CSs/EV placement is to reduce the overloading effect on the system and improve the performance of the system for the condition of EV penetration. By applying the optimization algorithm for this scenario, the CSs/EV best locations are at buses (2, 19 and 25). The real power losses have been reduced from 690.66 kW to 311.39 kW. There is a clear increase in voltage at bus 18 from 0.8886 p.u to 0.9011 p.u, and the voltage stability index is upgraded from 0.6172 to 0.6520 as shown in Figures 7 and 8 respectively, and the average voltage deviation index is decreased to 0.004041 from 0.0103. By observing the results, the losses have been reduced by 54.914% when compared to the losses in scenario 6 as shown in Table 4.

5.1.8. Scenario 8: Adding three max CS (450 EV) without optimal location

In this scenario, the total load has been incremented to 5023.50 kW (that is 2.35221 times more). Like scenario 2, losses have been increased to 1023.84 kW, that was 79.39% over the original case. The deviation index of voltage is increased to 0.01608, the stability index is reduced to 0.6172 and the lowest voltage on bus 18 failed to 0.8857 p.u as shown in Table 5.

Table 4. Performance indices comparison for 33- bus system (scenarios 1, 6 and 7)

System	Scenario	P-loss (kW)	VSI*min* (P.U)	V*min* (P.U)	AVDI (P.U)
33 buses	Scenario 1	210.99	0.67036	0.9042	0.00393
	Scenario 6	690.66	0.6172	0.8886	0.0103
	Scenario 7	311.39	0.6520	0.9011	0.00404

Figure 7. Voltage magnitude of 33- bus system with scenarios 1, 6 and 7

Figure 8. Voltage stability Index of 33-bus system with Scenarios 1, 6 and 7

Table 5. Performance indices comparison for 33- bus system (scenarios 8 and 9)

System	Scenario	P-loss (kW)	VSI*min* (P.U)	V*min* (P.U)	AVDI (P.U)
33 buses	Scenario 8	1023.84	0.6172	0.8857	0.01608
	Scenario 9	390.168	0.6546	0.8989	0.063777

5.1.9. Scenario 9: Adding three max CS (450 EV) with optimal location

Consequently, the results of applying the optimal location algorithm of the system with maximum EV penetration are at the positions (2, 19 and 25) as shown in Table 5. The real losses were reduced from 1023.8 kW to 390.168 kW, the low voltage on bus 18 increased from 0.8857 to 0.8989 p.u, the system stability index has improved from 0.6172 to 0.6546, and the mean deviation index reached 0.063777 from 0.01608. From the results, losses have been reduced by 61.89% when compared to the condition without the optimal sites for CSs/EV. Figures 9 and 10 indicate the profiles of the voltage and stability index for scenarios 8 and 9 respectively.
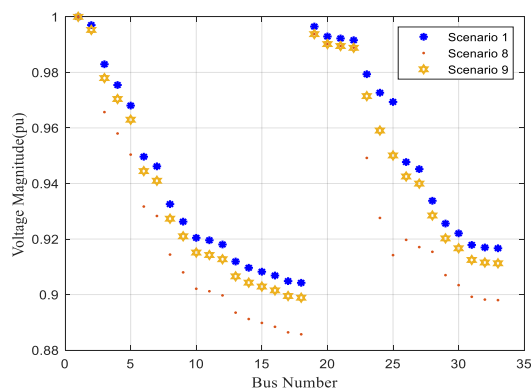

Figure 9. Voltage magnitude of 33- bus system with scenarios 1, 8 and 9
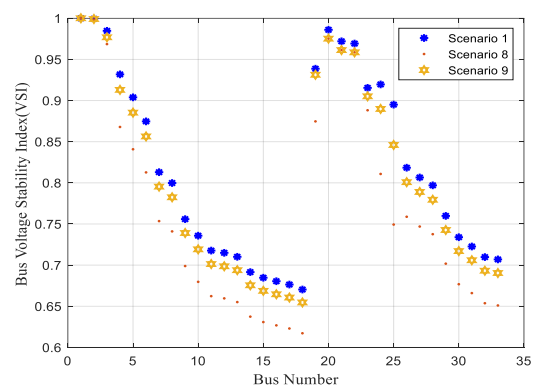

Figure 10. Voltage stability index of 33-bus system with scenarios 1, 8 and 9

Although the CSs/EV rated power are changed in the process of optimization in the chosen scenarios, the best locations of CSs/EV are the same for all optimization scenarios. Figures 11 and 12 indicate the bus voltage magnitude and stability index for all scenarios. The obtained results proved the

effectiveness of the proposed algorithm's in reducing the active power losses while minimizing the voltage deviation and improving the voltage stability index.

Since the CSs/EV rated power are the same in the process of optimization, the best locations of CSs/EVs are the same for all the mentioned algorithms in Table 6. Table 6 indicates a comparison of various algorithms for active power losses of lower, upper, and average values in the two optimization scenarios with minimum and maximum EV penetration. By observing the average value of objective function, the proposed algorithm (MOGA) outperformed TLBO, FPA, PSO, CSA, and ALO in all conditions with the best mean.
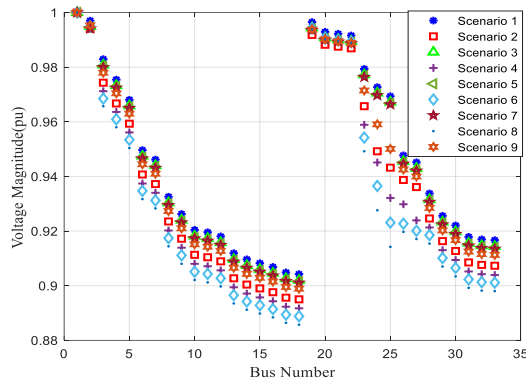
Figure 11. Voltage magnitude for all scenarios in 33-bus system
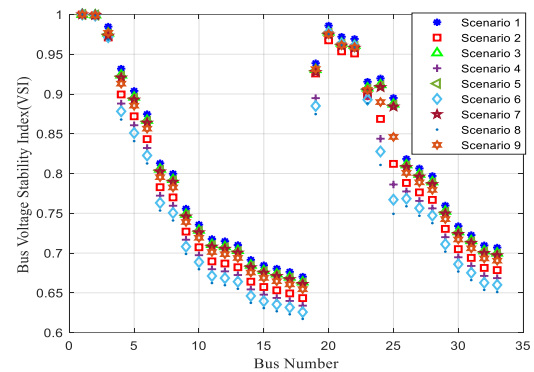
Figure 12. Voltage stability index for all scenarios in 33-bus system

Table 6. Characteristics of confluence of energy losses for various algorithms in 33 bus systems

Scheme	OF level	OF value for Different algorithms					
		MOGA	TLBO	FPA	PSO	CSA	ALO
Scheme 3	Minimum	Lower	279.1910	279.1910	279.1900	279.1910	279.1910	279.1910
	penetration	Upper	310.5340	311.8340	354.2120	375.1570	311.8340	330.3820
	of EV load	mean	279.0230	279.7760	298.3300	298.7520	298.6550	279.8550
Scheme 9	Maximum	lower	392.1990	392.1990	392.1980	392.9900	392.1990	392.1990
	penetration	upper	587.2700	588.3400	524.6200	583.2091	760.5141	720.2550
	of EV load	mean	397.1050	397.8240	402.0910	403.8210	412.0380	403.2560

5.2. Simulation results for IEEE 69-bus system depend on growth of EV load

The 69-bus system operates at 12.66 kV [37], with total load of 3801.40 kW as a real power and reactive power load is 2693.60 kVAR. The active and reactive power losses resulting from load flow are 224.881 kW and 102.1090 kVAR, respectively. Also, the minimum observed voltage at bus 65 is 0.9101 p.u and, the VSI at bus 65 is 0.6878 p.u.

Similar to the simulation of the 33-bus system, the three CSs/EV given in Table 1 are integrated into the tested system with and without applying the proposed algorithm. As the CSs/EV rated power is changed in the process of optimization in various chosen schemes, the CSs/EV are distributed in buses (2, 28 and 47) as the best location for all optimization schemes. Table 7 illustrated the results of all schemes of 69-bus system. Again, the results proved the effectiveness of the proposed algorithm for reducing the active power losses while minimizing the voltage deviation and improving the voltage stability index. But unlike 33-bus system, the optimization process returns the system to its original state, and hence the results are identical to the base case without connecting any car as shown in Figures 13 and 14. These figures indicate the stability index and the bus voltage magnitude.

Table 7. 69-bus system performance with penetration of EV load with and without optimal placing

| System	Scheme	load condition	P-loss (kW)	VSImin (P.U)	Vmin (P.U)	AVDI (P.U)
69 buses	Scheme 1	without EV load	224.881	0.6878	0.9101	0.00139
	Scheme 2	300 EV (without optimal place)	613.183	0.5695	0.8830	0.0034
	Scheme 3	300 EV (with optimal place)	225.0328	0.6878	0.9101	0.00139
	Scheme 4	350 EV (without optimal place)	625.28	0.5457	0.8241	0.00255
	Scheme 5	350 EV (with optimal place)	225.090	0.6878	0.9101	0.00139
	Scheme 6	400 EV (without optimal place)	804.240	0.5220	0.8486	0.00617
	Scheme 7	400 EV (with optimal place)	225.65	0.6878	0.9101	0.00139
	Scheme 8	max EV (without optimal place)	1108.41	0.3414	0.7637	0.0075
	Scheme 9	max EV (with optimal place)	225.4762	0.6878	0.9101	0.00139
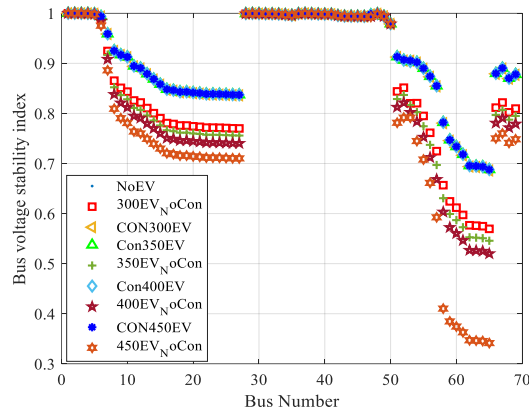
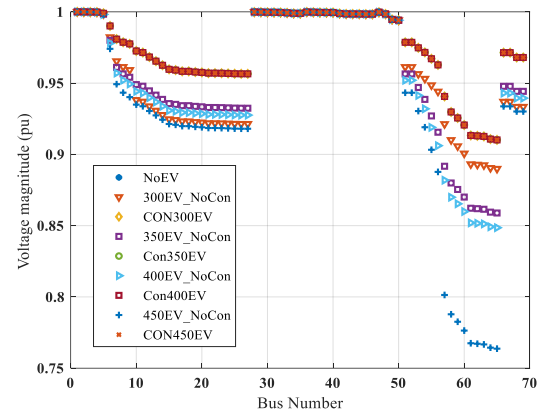Figure 13. Stability index in 69-bus system for all schemes

Figure 14. Voltage profile in 69-bus system for all schemes

6. CONCLUSION

A multi objective genetic algorithm was presented to formulate optimization problems for minimizing power-loss and improving the voltage stability index in the radial distribution systems. In addition, the voltage deviation index has been considered in order to enhance system stability and accelerate the determination process of detecting the optimal locations of EV charging stations (CS/EV). Different types of CSs as well as EVs were considered and integrated during the design process of the proposed algorithm. In addition, its application in standard IEEE systems is investigated. The optimal location of the CS/EV is observed to have a significant effect on the 33-bus system with losses increase of 39.81% for minimum penetration of EV and 84.83% for maximum EV penetration in comparison with the original operating condition of the system. But with the adoption of the optimal location of CSs/EV in 69-bus system, the technical interest required was nearly negligible when compared with the original load condition (without EV load). In addition, optimizing CS/EV allocation is depending on the performance of the distribution system. On the other hand, the algorithm demonstrated the ability to solve complex multi-objective nonlinear problem by consistently giving an objective value. It is worth noting that optimization with an intelligent EV charging feature significantly improves the performance of the system, and this will be the future field of research.

REFERENCES

[1] M. Zhang, X. Yuan, and J. Hu, "Inertia and Primary Frequency Provisions of PLL-Synchronized VSC HVDC When Attached to Islanded AC System," *IEEE Transactions on Power Systems*, vol. 33, no. 4, pp. 4179–4188, 2018, doi: 10.1109/TPWRS.2017.2780104.

[2] M. Z. Zeb *et al.*, "Optimal Placement of Electric Vehicle Charging Stations in the Active Distribution Network," *IEEE Access*, vol. 8, pp. 68124–68134, 2020, doi: 10.1109/ACCESS.2020.2984127.

[3] D. Meyer and J. Wang, "Integrating ultra-fast charging stations within the power grids of smart cities: A review," *IET Smart Grid*, vol. 1, no. 1, pp. 3–10, 2018, doi: 10.1049/iet-stg.2018.0006.

[4] M. Akbari, M. Brenna, and M. Longo, "Optimal locating of electric vehicle charging stations by application of Genetic Algorithm," *Sustainability (Switzerland)*, vol. 10, no. 4, 2018, doi: 10.3390/su10041076.

[5] M. Schmidt, P. Zmuda-trzebiatowski, M. Kiciński, P. Sawicki, and K. Lasak, "Multiple-criteria-based electric vehicle charging infrastructure design problem," *Energies*, vol. 14, no. 11, 2021, doi: 10.3390/en14113214.

[6] S. Shrestha and T. M. Hansen, "Distribution feeder impacts of electric vehicles charging in an integrated traffic and power network," *NAPS 2016 - 48th North American Power Symposium, Proceedings*, 2016, doi: 10.1109/NAPS.2016.7747888.

[7] V. K. B. Ponnam and K. Swarnasri, "Multi-Objective Optimal Allocation of Electric Vehicle Charging Stations and Distributed Generators in Radial Distribution Systems using Metaheuristic Optimization Algorithms," *Engineering, Technology & Applied Science Research*, vol. 10, no. 3, pp. 5837–5844, 2020, doi: 10.48084/etasr.3517.

[8] G. Andersson and D. I. M. G. Vaya, "The role of plug-in electric vehicles in system restoration after black-out," *Semester Thesis, EEH-Power Systemss Laboratory*, ETH Zurich, 2013.

[9] K. E. Adetunji, I. W. Hofsajer, A. M. Abu-Mahfouz, and L. Cheng, "A Review of Metaheuristic Techniques for Optimal Integration of Electrical Units in Distribution Networks," *IEEE Access*, vol. 9, pp. 5046–5068, 2021, doi: 10.1109/ACCESS.2020.3048438.

[10] Y. Zhang, Y. Wang, F. Li, B. Wu, Y. Y. Chiang, and X. Zhang, "Efficient Deployment of Electric Vehicle Charging Infrastructure: Simultaneous Optimization of Charging Station Placement and Charging Pile Assignment," *IEEE Transactions on Intelligent Transportation Systems*, vol. 22, no. 10, pp. 6654–6659, 2021, doi: 10.1109/TITS.2020.2990694.

[11] G. Alkawsi, Y. Baashar, U. Dallatu Abbas, A. A. Alkahtani, and S. K. Tiong, "Review of renewable energy-based charging infrastructure for electric vehicles," *Applied Sciences (Switzerland)*, vol. 11, no. 9, 2021, doi: 10.3390/app11093847.

[12]   A. A. Galadima, T. Aja Zarma, and M. A. Aminu, "Review on Optimal Siting of Electric Vehicle Charging Infrastructure," *Journal of Scientific Research and Reports*, pp. 1–10, 2019, doi: 10.9734/jsrr/2019/v25i1-230175.

[13]   H. Fredriksson, M. Dahl, and J. Holmgren, "Optimal placement of charging stations for electric vehicles in large-scale transportation networks," *Procedia Computer Science*, vol. 160, pp. 77–84, 2019, doi: 10.1016/j.procs.2019.09.446.

[14]   C. Bian, H. Li, F. Wallin, A. Avelin, L. Lin, and Z. Yu, "Finding the optimal location for public charging stations - A GIS-based MILP approach," *Energy Procedia*, vol. 158, pp. 6582–6588, 2019, doi: 10.1016/j.egypro.2019.01.071.

[15]   G. Napoli, A. Polimeni, S. Micari, G. Dispenza, and V. Antonucci, "Optimal allocation of electric vehicle charging stations in a highway network: Part 2. The Italian case study," *Journal of Energy Storage*, vol. 26, 2019, doi: 10.1016/j.est.2019.101015.

[16]   H. Zhang, L. Tang, C. Yang, and S. Lan, "Locating electric vehicle charging stations with service capacity using the improved whale optimization algorithm," *Advanced Engineering Informatics*, vol. 41, 2019, doi: 10.1016/j.aei.2019.02.006.

[17]   A. A. Londoño and M. Granada-Echeverri, "Optimal placement of freight electric vehicles charging stations and their impact on the power distribution network," *International Journal of Industrial Engineering Computations*, vol. 10, no. 4, pp. 535–556, 2019, doi: 10.5267/j.ijiec.2019.3.002.

[18]   W. Kong, Y. Luo, G. Feng, K. Li, and H. Peng, "Optimal location planning method of fast charging station for electric vehicles considering operators, drivers, vehicles, traffic flow and power grid," *Energy*, vol. 186, 2019, doi: 10.1016/j.energy.2019.07.156.

[19]   A. Shukla, K. Verma, and R. Kumar, "Multi-objective synergistic planning of EV fast-charging stations in the distribution system coupled with the transportation network," *IET Generation, Transmission and Distribution*, vol. 13, no. 15, pp. 3421–3432, 2019, doi: 10.1049/iet-gtd.2019.0486.

[20]   P. Rajesh and F. H. Shajin, "Optimal allocation of EV charging spots and capacitors in distribution network improving voltage and power loss by Quantum-Behaved and Gaussian Mutational Dragonfly Algorithm (QGDA)," *Electric Power Systems Research*, vol. 194, 2021, doi: 10.1016/j.epsr.2021.107049.

[21]   K. Kasturi and M. R. Nayak, "Assessment of techno-economic benefits for smart charging scheme of electric vehicles in residential distribution system," *Turkish Journal of Electrical Engineering and Computer Sciences*, vol. 27, no. 2, pp. 685–696, 2019, doi: 10.3906/elk-1801-34.

[22]   O. Beaude, S. Lasaulce, M. Hennebel, and J. Daafouz, "Minimizing the impact of EV charging on the electricity distribution network," *2015 European Control Conference, ECC 2015*, pp. 648–653, 2015, doi: 10.1109/ECC.2015.7330615.

[23]   O. Beaude, S. Lasaulce, M. Hennebel, and I. Mohand-Kaci, "Reducing the Impact of EV Charging Operations on the Distribution Network," *IEEE Transactions on Smart Grid*, vol. 7, no. 6, pp. 2666–2679, 2016, doi: 10.1109/TSG.2015.2489564.

[24]   L. G. González, E. Siavichay, and J. L. Espinoza, "Impact of EV fast charging stations on the power distribution network of a Latin American intermediate city," *Renewable and Sustainable Energy Reviews*, vol. 107, pp. 309–318, 2019, doi: 10.1016/j.rser.2019.03.017.

[25]   Y. Xia, B. Hu, K. Xie, J. Tang, and H. M. Tai, "An EV charging demand model for the distribution system using traffic property," *IEEE Access*, vol. 7, pp. 28089–28099, 2019, doi: 10.1109/ACCESS.2019.2901857.

[26]   P. Chittur Ramaswamy *et al.*, "Impact of electric vehicles on distribution network operation: Real world case studies," *IET Conference Publications*, vol. 2016, no. CP686, 2016, doi: 10.1049/cp.2016.0749.

[27]   P. V. K. Babu and K. Swarnasri, "Multi-objective optimal allocation of electric vehicle charging stations in radial distribution system using teaching learning based optimization," *International Journal of Renewable Energy Research*, vol. 10, no. 1, pp. 366–377, 2020, doi: 10.20508/ijrer.v10i1.10453.g7882.

[28]   S. Gao, H. Jia, J. Liu, and C. Liu, "Integrated configuration and charging optimization of aggregated electric vehicles with renewable energy sources," *Energy Procedia*, vol. 158, pp. 2986–2993, 2019, doi: 10.1016/j.egypro.2019.01.968.

[29]   K. Chaudhari, N. K. Kandasamy, A. Krishnan, A. Ukil, and H. B. Gooi, "Agent-based aggregated behavior modeling for electric vehicle charging load," *IEEE Transactions on Industrial Informatics*, vol. 15, no. 2, pp. 856–868, 2019, doi: 10.1109/TII.2018.2823321.

[30]   S. K. Injeti, "A Pareto optimal approach for allocation of distributed generators in radial distribution systems using improved differential search algorithm," *Journal of Electrical Systems and Information Technology*, vol. 5, no. 3, pp. 908–927, 2018, doi: 10.1016/j.jesit.2016.12.006.

[31]   K. Balu and V. Mukherjee, "Siting and Sizing of Distributed Generation and Shunt Capacitor Banks in Radial Distribution System Using Constriction Factor Particle Swarm Optimization," *Electric Power Components and Systems*, vol. 48, no. 6–7, pp. 697–710, 2020, doi: 10.1080/15325008.2020.1797935.

[32]   V. Janamala and T. K. S. Pandraju, "Static voltage stability of reconfigurable radial distribution system considering voltage dependent load models," *Mathematical Modelling of Engineering Problems*, vol. 7, no. 3, pp. 450–458, 2020, doi: 10.18280/mmep.070316.

[33]   J. Jin, L. Rothrock, P. L. McDermott, and M. Barnes, "Using the analytic hierarchy process to examine judgment consistency in a complex multiattribute task," *IEEE Transactions on Systems, Man, and Cybernetics Part A:Systems and Humans*, vol. 40, no. 5, pp. 1105–1115, 2010, doi: 10.1109/TSMCA.2010.2045119.

[34]   M. Krajčovič, V. Hančinskỳ, L. Dulina, P. Grznár, M. Gašo, and J. Vaculík, "Parameter setting for a genetic algorithm layout planner as a toll of sustainable manufacturing," *Sustainability (Switzerland)*, vol. 11, no. 7, 2019, doi: 10.3390/su1102083.

[35]   D. Devaraj, "Improved genetic algorithm for multi-objective reactive power dispatch problem," *European Transactions on Electrical Power*, vol. 17, no. 6, pp. 569–581, 2007, doi: 10.1002/etep.146.

[36]   D. Q. Hung and N. Mithulananthan, "Multiple Distributed Generator Placement in Primary Distribution Networks for Loss Reduction," *IEEE Transactions on Industrial Electronics*, vol. 60, no. 4, pp. 1700–1708, Apr. 2013, doi: 10.1109/TIE.2011.2112316.

[37]   J. S. Savier and D. Das, "Impact of network reconfiguration on loss allocation of radial distribution systems," *IEEE Transactions on Power Delivery*, vol. 22, no. 4, pp. 2473–2480, 2007, doi: 10.1109/TPWRD.2007.905370.

[38]   O. Ouramdane, E. Elbouchikhi, Y. Amirat, and E. S. Gooya, "Optimal sizing and energy management of microgrids with Vehicle-to-Grid technology: A critical review and future trends," *Energies*, vol. 14, no. 14, 2021, doi: 10.3390/en14144166.

[39]   F. Mwasilu, J. J. Justo, E. K. Kim, T. D. Do, and J. W. Jung, "Electric vehicles and smart grid interaction: A review on vehicle to grid and renewable energy sources integration," *Renewable and Sustainable Energy Reviews*, vol. 34, pp. 501–516, 2014, doi: 10.1016/j.rser.2014.03.031.

BIOGRAPHIES OF AUTHORS

Afaf Rabie 🆔 🔬 SC ℧ received the B.Sc. and M.Sc. degrees from Mansoura University, Mansoura, Egypt, in 2006 and 2012, respectively, all in electrical engineering. She is currently pursuing the Ph.D. degree in electrical engineering with the Mansoura University, Egypt. She currently works with North Delta Electricity Distribution Co., Mansoura, Egypt. Her research interests include Stability analysis in weak grids, grid connected electric vehicles and distributed optimization. She can be contacted at email: afaf_fathy2006@yahoo.com.

Abdelhady Ghanem 🆔 🔬 SC ℧ received the B.Sc., M.Sc., and Ph.D. degrees from Mansoura University, Mansoura, Egypt, in 2006, 2011, and 2017, respectively, all in electrical engineering. Since 2006, he has been with the Electrical Engineering Department, Mansoura University, where he is now an Associate Professor. He joined the University of Nottingham, Nottingham, U.K., as an Occasional Ph.D. Student (Joint Supervision Scheme between Mansoura University and the University of Nottingham), from February 2015 to May 2017. His research interests include electrical systems modeling, renewable power generation, power system analysis and control, grid-connected power electronics converters, fault diagnosis, and stability analysis. He can be contacted at email: aghanem_m@mans.edu.eg.

Sahar S. Kaddah 🆔 🔬 SC ℧ received her B.Sc. (1988) and M.Sc. (1992) from Mansoura University, Egypt. She received her Ph.D. from Howard University, Washington, DC, USA, in 2002. She has been a professor at the Electrical Engineering Department, Mansoura University since 2017. Her research interests are the analysis and control of power systems, renewable energy applications, DG, microgrids, and power system optimization. She can be contacted at email: skaddah@mans.edu.eg.

Magdi M. El-Saadawi 🆔 🔬 SC ℧ was born in Mansoura, Egypt, in 1959. He received the B.Sc. and M.Sc. degrees from Mansoura University, Egypt, in 1982 and 1988, respectively, and the Ph.D. degree from the Warsaw University of Technology, in 1997. He was a Teaching Assistant with El-Mansoura University from 1983– 1992. From 1997, he was a Staff Member with the Electrical Engineering Department, Mansoura University, and has been a Professor since May 2011. He was the Head of the Electrical Engineering Department, Mansoura University from 2011 to 2012. His research interests include renewable energy, distributed generation, and power system analysis. He can be contacted at email: m_saadawi@mans.edu.eg.